On the Precipitation-Strengthening Contribution of the Ta-Containing $Co_3(Al,W)$-Phase to the Creep Properties of γ/γ' Cobalt-Base Superalloys

A. BEZOLD, N. VOLZ, F. XUE, C.H. ZENK, S. NEUMEIER, and M. GÖKEN

The creep strength of single-crystalline Co-based superalloys was found to be comparable to first-generation Ni-base superalloys. However, considerable shearing of the γ' precipitates was observed in the early creep stages. To determine the strengthening contribution of the Ta-containing γ'-$Co_3(Al,W)$ precipitates, the creep strength of several single-crystalline Co-Al-W-Ta superalloys was determined as a function of the γ' volume fraction at 1223 K (950 °C) and stress levels between 25 and 600 MPa. Employing a Lagneborg–Bergman–Reppich (LBR) approach, it is found that the strengthening contribution of the γ' precipitates increases significantly with increasing γ' volume fraction. In a Co-base superalloy that exhibits a precipitate volume fraction of about 70 pct, the γ'-strengthening contribution calculated with the LBR approach ranges between the ones observed in first-generation Ni-base superalloy CMSX-6 and second-generation Ni-base superalloy CMSX-4.

https://doi.org/10.1007/s11661-020-05626-2

I. INTRODUCTION

ABOUT a decade ago, investigations of the ternary Co-Al-W system revealed the existence of the intermetallic γ'-$Co_3(Al,W)$ phase.[1] Since then, numerous studies concluded that in particular Ta is a key alloying element for Co-base superalloys as it strongly partitions to the γ' precipitates[2–4] and thereby stabilizes the γ' phase,[4–7] increases the γ' solvus temperature,[2,5–7] the γ' volume fraction,[4,6] the superlattice intrinsic stacking fault (SISF) energy[8,9] and the hardness of the γ' precipitates.[4] The beneficial effect of Ta additions to ternary Co-Al-W superalloys was also observed in compression and creep experiments.[5,10–14] The Ta-containing alloys showed a significant increase in yield and creep strength. Furthermore, Ta-containing single-crystalline (SX) Co-Al-W superalloys showed a creep strength comparable to first-generation Ni-base superalloys in the intermediate temperature/stress regime (*e.g.* 1173 K (900 °C)/350 MPa) under tensile creep.[10] Microstructural investigations of interrupted tensile creep specimens by Titus *et al.*[15] revealed that the γ' precipitates in a quaternary Co-8.8Al-9.8W-2Ta SX superalloy were considerably sheared after less than one percent plastic strain at 1173 K (900 °C)/350 MPa. Shearing of the γ' precipitates was also reported in a quaternary Co-9Al-7.5W-2Ta SX superalloy after 0.5 pct plastic strain under a compressive load of only 150 MPa at a temperature of 1223 K (950 °C).[16] Recently, Lenz *et al.*[17] studied the tension–compression asymmetry in a CoNi-base superalloy at 1123 K (850 °C) and 400 MPa. Even though the shearing mechanisms differ depending on the sign of the applied load, the authors calculated that nearly 10 pct of the total plastic creep strain of 0.3 pct can be attributed to shearing events in the γ' precipitates for both tensile and compressive creep. Thus, the plastic strain contribution of the shearing of the γ' precipitates is substantial but not dominant at these conditions. In contrast, the γ' precipitates in Ni-base superalloys are only sheared at a higher strain in the intermediate temperature/stress regime under tensile creep.[18–20]

To address the question how Co-base and Ni-base superalloys compare with respect to the γ' strengthening contribution, quaternary SX Co-Al-W-Ta superalloys with varying γ' volume fraction were crept at 1223 K

A. BEZOLD is with the Friedrich-Alexander-University Erlangen-Nürnberg, Department of Materials Science & Engineering, Institute I: General Materials Properties, Martensstr. 5, 91058, Erlangen, Germany and Friedrich-Alexander-University Erlangen-Nürnberg, Elite Master's Programme in Advanced Materials and Processes (MAP), Immerwahrstr. 2a, 91058, Erlangen, Germany. Contact e-mail: andreas.bezold@fau.de N. VOLZ is with the Friedrich-Alexander-University Erlangen-Nürnberg, Department of Materials Science & Engineering, Institute I: General Materials Properties. F. XUE is with Northwestern University, Department of Materials Science and Engineering, NUCAPT, 2220 North Campus Drive, Evanston, IL 60208 C. H. ZENK is with the Ruhr-University Bochum, Institute for Materials, Chair for Materials Science and Engineering, Universitätsstr. 150, 44801, Bochum, Germany S. NEUMEIER and M. GÖKEN are with the Friedrich-Alexander-University Erlangen-Nürnberg, Department of Materials Science & Engineering, Institute I: General Materials Properties.

Manuscript submitted 23 September 2019.
Article published online January 21, 2020

(950 °C) and compared to first- and second-generation Ni-base superalloys. Subsequently, an approach by Lagneborg and Bergman,[21] which was later extended by Reppich *et al.*,[22] was used to determine the γ' strengthening contribution, which is introduced in the following.

II. LAGNEBORG–BERGMAN–REPPICH APPROACH

The threshold stress σ_P (P for *precipitate*, also termed friction or back stress) was introduced by Lagneborg[23] and the group of Wilshire[24] into the traditional power law equation to rationalize the stress exponent n and activation energy Q of precipitation-strengthened alloys. These values are in general significantly higher, *e.g.* $n = 8.6$ and $Q = 740$ kJ/mol for a boron-containing γ/γ' Co-Al-W alloy,[11] than the theoretically derived values for metals or solid solutions, *i.e.* $n = 3$–5 and Q equal to the activation energy for self-diffusion Q_{SD}.[25] It is assumed that deformation occurs predominantly in the matrix phase below an effective stress of $(\sigma - \sigma_P)$.[24] The stress σ to produce a certain minimum creep rate $\dot{\varepsilon}_{min}$ in a precipitate-strengthened alloy at a given temperature can be expressed as a linear combination of the stress σ_M (that would produce the same creep rate in a single phase matrix alloy) and the strengthening contribution of the precipitates σ_P:[22]

$$\sigma = \sigma_M + \sigma_P \qquad [1]$$

Thus, the modified power law equation can be expressed as follows:

$$\dot{\varepsilon}_{min} = A(\sigma - \sigma_P)^{n_M} \exp\left(-\frac{Q_{SD}}{RT}\right), \qquad [2]$$

where A is a constant, σ is the applied stress, n_M is the stress exponent of the pure matrix phase, R is the universal gas constant and T is the temperature.

Lagneborg and Bergman[21] introduced an approach to derive the precipitation strengthening contribution for various stress values $\sigma_P(\sigma)$ from creep experiments at a given temperature by replotting the Norton plot with linearly scaled axes and with the n_M-th root of the minimum creep rate over the applied stress, compare Figures 1(a) and (b). The resulting threshold stress diagram (see Figure 1(c)) can be distinguished in two characteristic regimes:[21,26]

(1) $\sigma_P = \sigma_{P,max} = \text{const}: \sigma_{P,max}$ is determined by the intersection of the x-axis and the linear extrapolation of the high stress branch (see Figure 1(b)). In this regime, σ_P is assumed to represent the additional stress for shearing or the Orowan process[26] and is therefore constant (see Figure 1(c)).

2) $\sigma_P = K_{LB}\sigma$: The proportionality constant K_{LB} can be derived by the slope K of the low stress branch in Figure 1(b).[21] The dominating deformation mechanism in regime 2 is predominantly climb of dislocations.[26]

While this procedure provides a rough estimate of $\sigma_P(\sigma)$, several issues have to be addressed to determine $\sigma_P(\sigma)$ more accurately: n_M and σ_P are generally not constant at the same time.[22] Additionally, $\sigma_M(\dot{\varepsilon}_{min})$ has to be known to accurately determine K_{LB}, since K_{LB} strongly depends on the ratio of σ_M to σ due to the superposition rule:

$$K_{LB} = \frac{\Delta\sigma_P(\dot{\varepsilon}_{min})}{\Delta\sigma(\dot{\varepsilon}_{min})} = 1 - \frac{\Delta\sigma_M(\dot{\varepsilon}_{min})}{\Delta\sigma(\dot{\varepsilon}_{min})} \qquad [3]$$

Therefore, Reppich *et al.*[22] modified the approach of Lagneborg and Bergman by considering the creep data of the corresponding matrix phase, where the stress dependence of $\dot{\varepsilon}_{min}$ is described by the following equation after Blum and Reppich:[27]

$$\dot{\varepsilon}_{min} = B\sigma^{n^*-1}\sinh\left(\frac{V_{app}\sigma}{2kT}\right), \qquad [4]$$

where B is a constant, n^* is the effective, constant stress exponent at low stress levels, V_{app} is the apparent activation volume, k is the Boltzmann constant and T is the temperature. The effective stress exponent n_M of Eq. [4] can be derived as follows:[27]

$$n_M = \left(\frac{\partial \ln(\dot{\varepsilon}_{min})}{\partial \ln(\sigma)}\right)_T = n^* - 1 + \frac{V_{app}\sigma}{2kT}\coth\left(\frac{V_{app}\sigma}{2kT}\right) \qquad [5]$$

Note that at a stress below the matrix power law breakdown (PLB), $\coth(V_{app}\sigma/2kT)$ can be approximated with $2kT/V_{app}\sigma$, which leads to a constant stress exponent $n_M = n^*$ consistent with the power law equation (see Figure 1(d)).[22] Since n_m increases at higher stress levels, the curves of the matrix and the precipitation-strengthened alloy in the $\dot{\varepsilon}_{min}^{1/n_M}$ vs. σ plot are no longer linear but change to a convex curvature (see Figure 1(e)).[22] Due to the superposition rule (Eq. [1]), $\sigma_P(\dot{\varepsilon}_{min})$ can simply be derived by subtracting $\sigma_M(\dot{\varepsilon}_{min})$ from $\sigma(\dot{\varepsilon}_{min})$. The slope of regime 2 of the resulting $\sigma_P(\sigma)$ diagram (see Figure 1(f)) complies with Eq. [3].

III. EXPERIMENTAL METHODS

The compositions of the γ and γ' phases of a Co-9Al-7.5W-2Ta alloy with a γ' volume fraction of approximately 50 pct[16] were determined by atom probe topography after aging at 1173 K (900 °C) for 200 hours. By changing the alloy compositions along the resulting γ/γ' tie-line, the investigated alloys were designed to vary only in the γ' volume fraction. Master alloys with the composition of the γ and γ' phases (Master alloy A and Master alloy B (see Table I)) were cast at *Mateck GmbH* using raw elements with a purity of at least 99.9 pct. Subsequently, both master alloys were mixed to create an alloy series, called

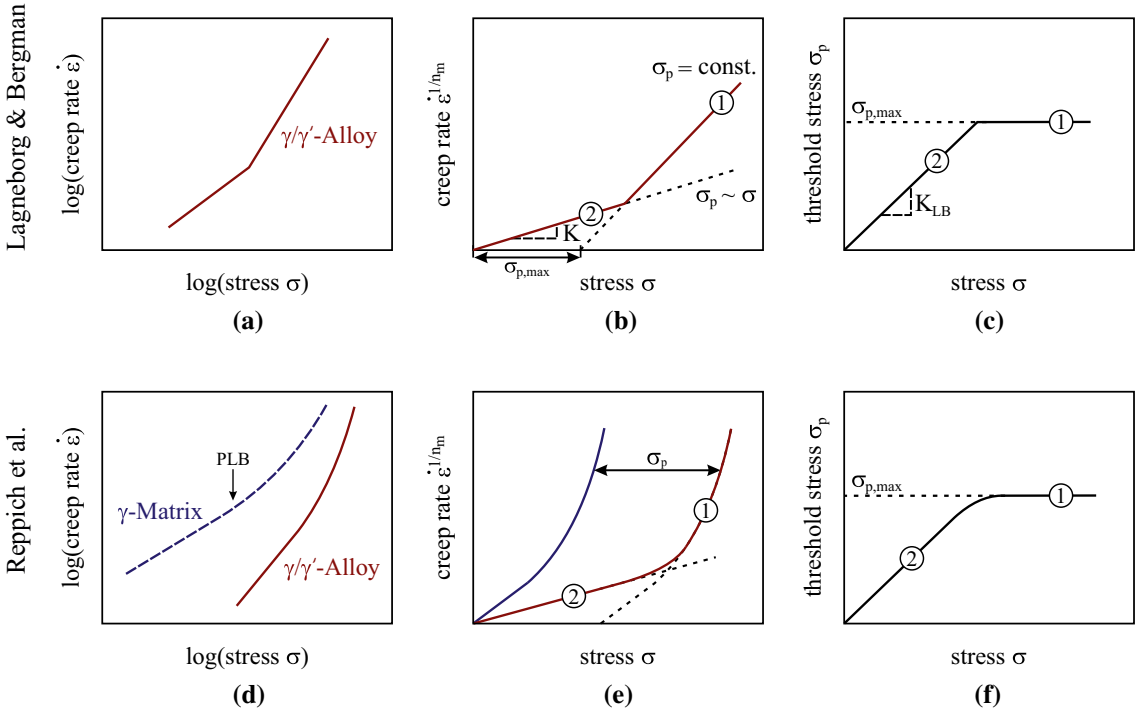

Fig. 1—Schematic diagrams of the procedure for the determination of the precipitation strengthening contribution (threshold stress) (*a*), (*b*), (*c*) after Lagneborg and Bergman[21] and the (*d*), (*e*), (*f*) modified procedure after Reppich *et al.*[22]

Table I. Nominal and Measured Composition of the Investigated Alloys of the ERBOCo-VF Alloy Series and the Master Alloys in Atomic Percent

	Nominal/Measured Composition in Atomic Percent			
Alloy	Co	Al	W	Ta
VF0/Master Alloy A	86.7/87.3	8.8/8.4	4.0/4.1	0.5/0.2
VF20	84.4/84.8	8.8/8.6	5.7/6.0	1.1/0.6
VF40	82.1/82.7	8.9/8.5	7.3/7.7	1.7/1.1
VF60	79.8/80.7	8.9/8.4	9.0/9.3	2.3/1.6
Master Alloy B	75.2/77.0	9/8.1	12.3/12.5	3.5/2.4

ERBOCo-VF. The respective alloy designation contains their intended γ' volume fraction, *e.g.* "VF20" for an alloy with an intended γ' volume fraction of 20 pct (see Table I for alloy compositions). The alloys were cast in a laboratory scale Bridgman furnace using a withdrawal rate of 3 mm/min at an estimated temperature gradient of about 5 K/mm after holding the melt at 1823 K (1550 °C) for five minutes (for further details about the equipment see Reference 28). The resulting rods had a length of 120 mm and a diameter of 12 mm. The single-crystalline bars were solution heat treated at 1623 K (1350 °C) for 24 h and aged at 1173 K (900 °C) for 100 h in a vacuum furnace. Further details on the design, microstructure and thermophysical properties of the ERBOCo-VF alloy series will be published in a subsequent work.

Microstructural characterization was conducted on a *Zeiss Crossbeam 1540 EsB* scanning electron microscope (SEM) using a backscattered electron detector (BSE). The actual compositions of the alloys and master alloys were determined by energy-dispersive X-Ray spectroscopy (EDS) using the same device (see Table I). Misorientations smaller than 5 deg for VF20, VF40 and VF60 and of 11.6 deg for VF0 were determined by EBSD. The standard sample preparation for SEM investigations consisted of grinding up to 4000 grit, polishing using diamond suspension up to 1 μm and chemo-mechanical polishing using *Struers OPU*.

Cylindrical compressive creep specimens with a length of 7.5 mm and a diameter of 5 mm were produced by electric-discharge machining parallel to the solidification direction. Compressive creep experiments were performed in air at a temperature of 1223 K (950 °C) and at constant stress levels between 25 and 600 MPa. The creep tests were either interrupted at a plastic creep strain of 7 pct or after reaching the minimum creep rate for the longer lasting experiments.

IV. RESULTS

A. *Microstructure*

The microstructures of the investigated alloys after aging are shown in Figure 2. No additional phases except γ and γ' are found. The γ' volume fraction of the precipitation-strengthened alloys increases from 20 ± 4 pct for VF20 to 50 ± 1 pct for VF40 and 70 ± 2 pct for VF60 according to image analysis of the SEM-BSE micrographs, which have been stereographically corrected to obtain the volume fraction from the measured area fraction.[29] The γ' precipitates exhibit a cuboidal morphology and increase in size with increasing γ' volume fraction to an average edge length of 123 ± 35 nm, 166 ± 49 nm and 269 ± 64 nm for VF20, VF40 and VF60, respectively.

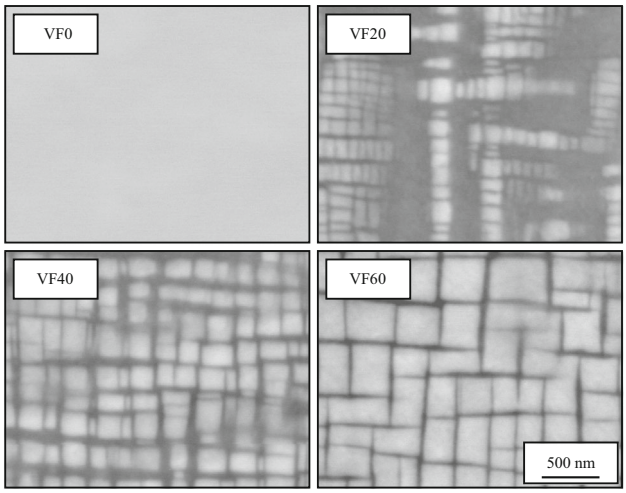

Fig. 2—SEM-BSE micrographs of the investigated SX Co-base superalloys after solution heat treatment for 24 h at 1623 K (1350 °C) and aging for 100 h at 1173 K (900 °C).

B. *Creep*

Creep curves of the alloys VF0 and VF60 are shown in Figure 3 for various stress levels. The matrix alloy VF0 exhibits a pronounced hardening regime after primary creep at a stress below 50 MPa. Thus, the minimum creep rate is only reached at higher plastic strain values. This degree of deformation obviously exceeds the strain in the matrix phase of the two-phase γ/γ' superalloys VF20, VF40 and VF60 at the minimum creep rate. Therefore, the creep rate at 1 pct plastic strain is used for VF0 for further calculations. The choice of the plastic strain, from which the creep rates of VF0 are taken, does not influence the results significantly as will be shown in the discussion.

The Norton plot (Figure 4) reveals that the creep strength increases with increasing γ' volume fraction over the investigated stress range. Here and also for the subsequent LBR approach, the creep rate at the first minimum is used for creep curves, which exhibit two minima (*i.e.* VF60 at 1223 K (950 °C) and 200 MPa (see Figure 3(b)). Since only the second creep minimum is associated with the completion of rafting at temperatures above 1223 K (950 °C)[16,30] and the first minimum is reached after a plastic strain of less than 0.5 pct, the effect of rafting is considered negligible in the following. By fitting Eq. [4] to the data of VF0, an apparent activation volume V_{app} of 76 b^3 is obtained (assuming deformation in the fcc crystal structure by full $a/2\ \langle 110 \rangle$ dislocations and a lattice parameter of 0.3637 nm as reported by Xue *et al.*[16] for the γ phase of Co-9Al-7.5W-2Ta at 1223 K (950 °C)). This value is higher than the one from the γ matrix of the Ni-base superalloy CMSX-4 with 36 b^3 and similar to the one of Nimonic 75 with 70 b^3 at 1223 K (950 °C).[31]

V. DISCUSSION

Using the procedure described by Reppich *et al.*,[22] the Lagneborg–Bergman–Reppich (LBR) plot (see Figure 5a) and the resulting precipitation strengthening

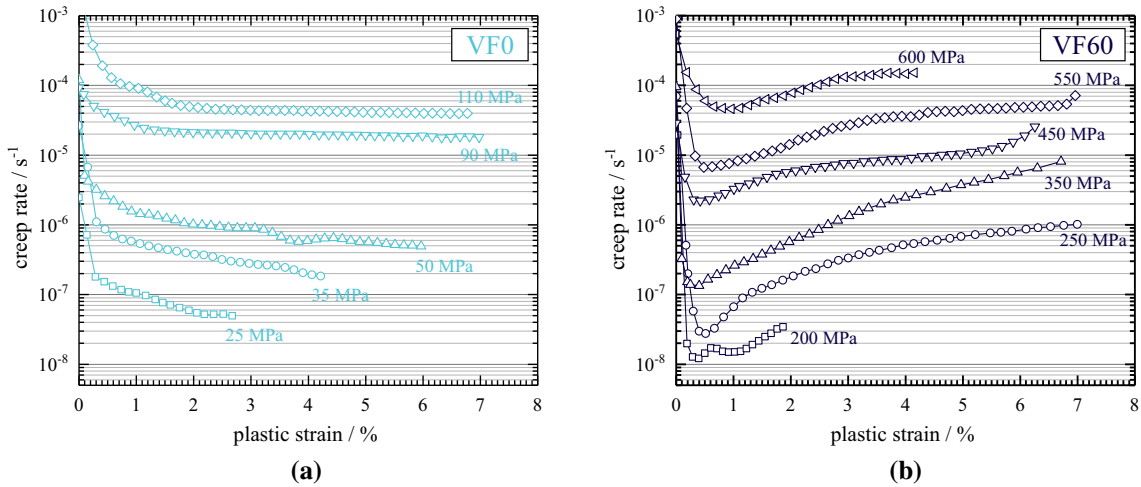

Fig. 3—Creep curves of the alloys (*a*) VF0 and (*b*) VF60 at 1223 K (950 °C) and various true stress levels.

diagram (see Figure 5(b)) can be obtained. As clearly seen in Figure 5(a), the LBR model describes the acquired creep data very well. However, Figure 5(b) shows that only VF20 exhibits a constant σ_P value of 121 MPa in regime 1. The slopes of the curves for VF40 and VF60 also decrease at a higher stress but do not converge to a constant value, even though the highest applied stress levels correspond to a minimum creep rate of almost 1×10^{-4} s^{-1}. The absence of a constant, maximum precipitation strengthening contribution was also determined by Schneider *et al.*[32] using the LBR approach for the Ni-base superalloy CMSX-4, which exhibits a γ' volume fraction of approximately 70 pct.

Based on these results, however, it cannot be concluded that no shearing is present. As a matter of fact, Xue *et al.* observed shearing of the γ' precipitates after less than 0.5 pct plastic strain at 1223 K (950 °C) and a stress of only 150 MPa in the Ta-containing SX Co-base superalloy, from which the VF-series is derived.[16] Despite the expected shearing for even the lowest applied stress values in this study, the initially nearly linear slopes in Figure 5(b) suggest that the majority of the deformation is still concentrated in the γ matrix. Recently, Lenz *et al.*[17] and Titus *et al.*[9] determined the contribution of γ' shearing to the plastic strain for CoNi-base superalloys and Co-base superalloys in compressive and tensile creep at 1123 K (850 °C)/400 MPa and 1173 K (900 °C)/345 MPa, respectively. These authors calculated that the contribution of shearing events is substantial but not dominant, which is qualitatively similar to the results in this study especially when the higher temperature of 1223 K (950 °C) and the lower stress levels between 200 and 300 MPa in the linear part of VF60 in Figure 5(b) are considered. At higher stress values the decreasing slope implies an increase in the contribution of shearing events to the total plastic strain. The absence of a constant, maximum γ'-strengthening contribution in VF40 and VF60 suggests that the glide-climb motion of dislocations in the γ matrix still plays an important role for a stress as high as 600 MPa. However, work hardening of the γ' precipitates due to the interaction of stacking faults as proposed by Titus *et al.*[9] could also play a significant role. Detailed TEM investigations are clearly necessary to explain the missing plateau in these alloys.

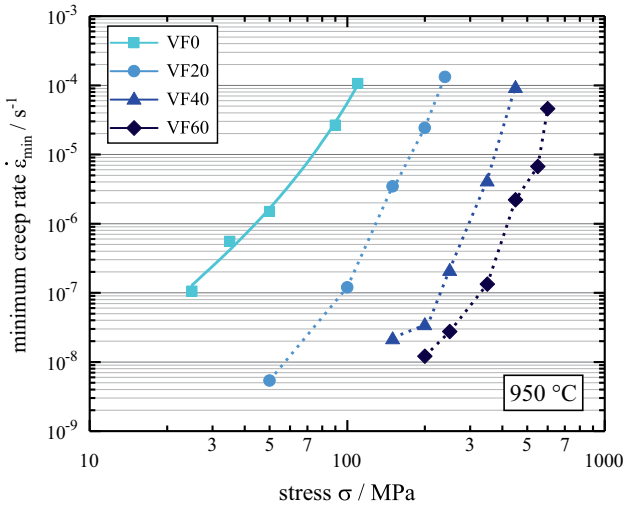

Fig. 4—Norton plot of the investigated SX Co-base superalloys tested at 1223 K (950 °C). The creep data of VF0 is fitted by Eq. [4]. The data points of VF20, VF40 and VF60 are connected for visual assistance.

These results indicate that the strengthening contribution of the γ' precipitates in Co-base superalloys calculated with the LBR approach—especially for alloys with a γ' volume fraction above 50 pct—cannot be easily distinguished in two characteristic regimes and the associated deformation mechanisms as described in the background section. Nevertheless, the LBR approach is still a valuable tool to calculate the precipitation strengthening contribution of an alloy for various stresses and minimum creep rates.

The precipitation strengthening diagram (see Figure 5(b)) is not ideal to compare different alloys especially at lower minimum creep rates because the

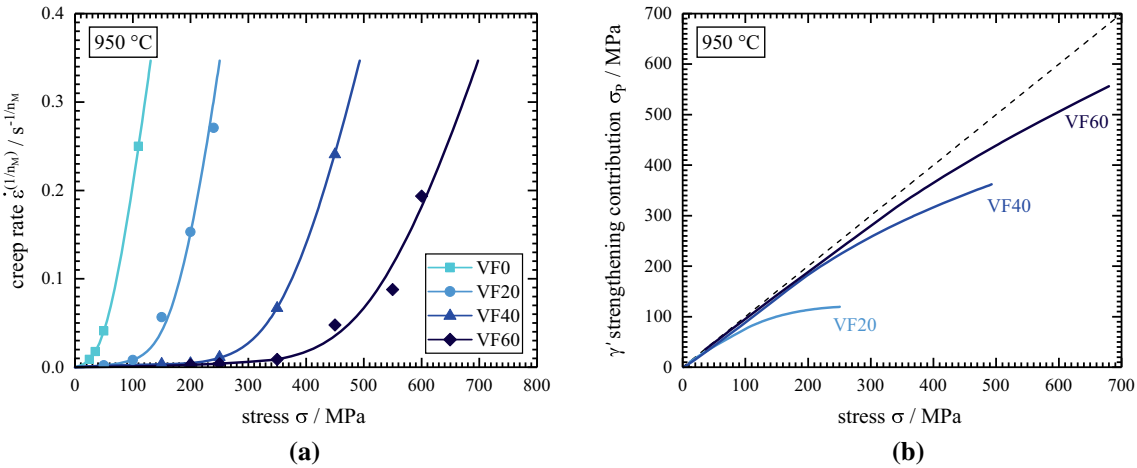

Fig. 5—(*a*) Lagneborg–Bergman–Reppich plot and (*b*) the resulting precipitation strengthening diagram of the investigated SX Co-base superalloys at 1223 K (950 °C).

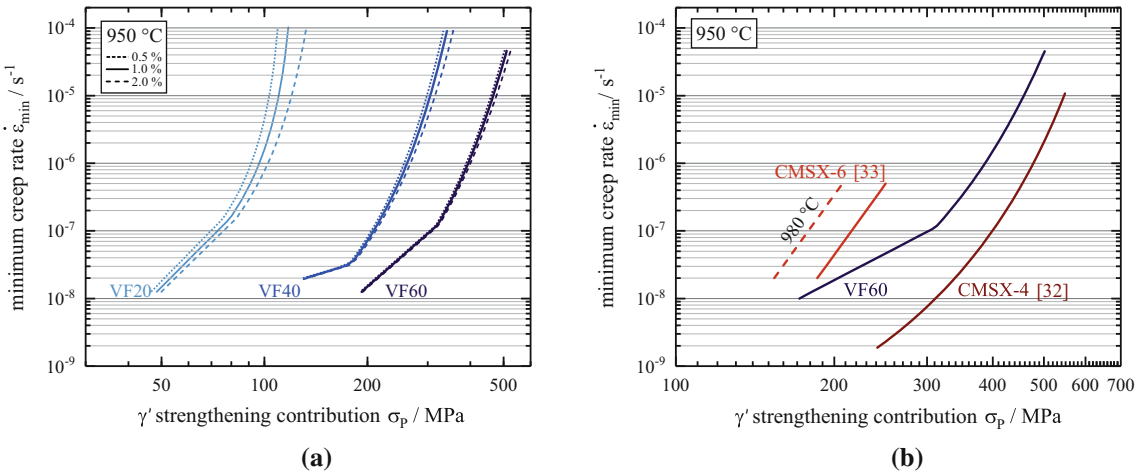

Fig. 6—The calculated strengthening contribution of the γ' precipitates in dependence of the minimum creep rate. (*a*) For the investigated γ'-strengthened Co-base superalloys and different plastic strain values, from which the creep rates of the matrix alloy VF0 are taken. (*b*) For VF60 in comparison with the Ni-base superalloys CMSX-6[33] and CMSX-4.[32] The dashed line for CMSX-6 indicates the original strengthening contribution determined at 1253 K (980 °C) in Reference 33, while the solid line represents an estimation at 1223 K (950 °C).

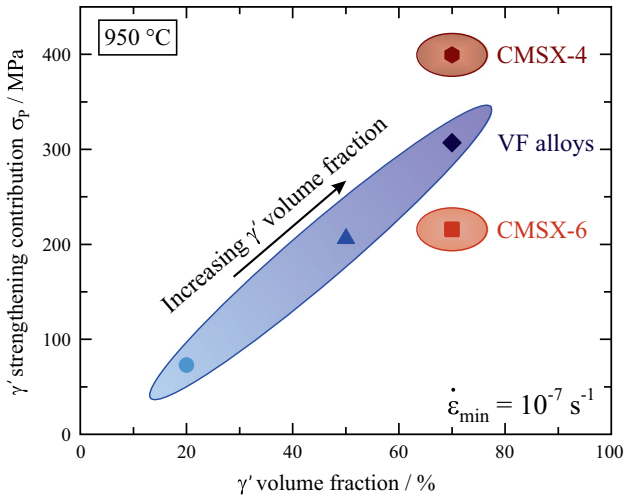

Fig. 7—The calculated strengthening contribution of the γ' precipitates in the Co-base superalloys VF20, VF40 and VF60 compared to that in the first- and second-generation Ni-base superalloys CMSX-6 and CMSX-4 in dependence of the γ' volume fraction at a temperature of 1223 K (950 °C) and at a minimum creep rate of 10^{-7} s^{-1}.

slope in regime 2 is only dependent on the ratio of the corresponding matrix stress σ_M to the applied stress σ (compare Eq. [3]). By plotting the minimum creep rate over the precipitation-strengthening contribution σ_P of the corresponding applied stress as shown in Figure 6(a), it can be seen that σ_P increases with increasing γ' volume fraction. In this study, the highest strengthening contribution is reached by VF60 with a γ' volume fraction of 70 pct.

The choice of the strain value, from which the creep rates of VF0 are taken, leads only to small differences for σ_P (see Figure 6(a)). At a minimum creep rate of 10^{-4} s^{-1}, these differences amount to less than 15 MPa, if the creep rates at a plastic strain of 0.5 or 2 pct are used to calculate σ_P. Additionally, this change is reduced to 6 MPa at a lower minimum creep rate of 10^{-7} s^{-1}.

In Figure 6(b), σ_P of the γ' precipitates in VF60 is compared with that in the first-generation Ni-base superalloy CMSX-6[33] and the second-generation Ni-base superalloy CMSX-4.[32] These alloys exhibit a similar γ' volume fraction and only a slightly larger γ' precipitate size of 440 nm and 470 nm, respectively, as compared to 269 nm in VF60.[32,34] Additionally, it has to be noted that the strengthening contribution in the study of Wilhelm *et al.*[33] was initially determined at 1253 K (980 °C), which was converted to 1223 K (950 °C) as shown in Appendix A. Figure 6(b) reveals that σ_P of the γ' precipitates in CMSX-4 is significantly increased compared to CMSX-6 at 1223 K (950 °C). Furthermore, it can be concluded that σ_P in VF60 ranges between the ones observed in the Ni-base superalloys CMSX-6 and CMSX-4 for all investigated minimum creep rates according to the LBR approach.

At a minimum creep rate of 10^{-7} s^{-1}, σ_P increases linearly with the γ' volume fraction for the investigated Co-base superalloys (see Figure 7). The slope corresponds to approximately 48 MPa per 10 pct γ' volume fraction. In comparison with the Ni-base superalloys, the calculated γ'-strengthening contribution in VF60 is about 90 MPa lower and higher than that in CMSX-4 and CMSX-6, respectively.

In contrast to both Ni-base superalloys, σ_P was determined in compressive creep tests in this study. The creep behavior of Ni-base superalloys is typically inferior under compressive stress compared to tensile stress for [001] oriented specimens in the low-temperature and high-stress regime (*i.e.* 1023 K (750 °C) and 750 MPa).[35–37] This asymmetry is explained by pronounced mechanical twinning in compressive creep.[35–37] In the intermediate temperature and stress regime (*i.e.* 1173 K to 1223 K (900 °C to 950 °C) and 250 to 392 MPa), the minimum creep rates are similar for both loading modes, even though larger primary creep strain values

are obtained under compressive creep.[36–38] Recently, Lenz *et al.*[17] observed slightly higher creep rates in a CoNi-base superalloy during tensile creep compared to compressive creep at 1123 K (850 °C) and 400 MPa. If a similar anisotropy is also present for the investigated alloys at the higher temperature of 1223 K (950 °C) and considering a negligible anisotropy for the Ni-base superalloys regarding the minimum creep rate, the obtained σ_P values would decrease slightly and σ_P of VF60 would get closer to that in CMSX-6. Despite these promising results, it has to be noted that VF60 is not optimized for harsh, corrosive environments compared to the complex, commercial Ni-base superalloys. However, further improvements of the creep properties are to be expected by optimized alloying additions, since VF60 represents only a quaternary model alloy.

VI. SUMMARY AND CONCLUSION

The strengthening contribution of the γ'-Co_3(Al,W,Ta) precipitates in Ta-containing single-crystalline Co-Al-W superalloys with varying γ' volume fraction was determined using a Lagneborg–Bergman–Reppich approach at 1223 K (950 °C). The following conclusions can be drawn:

- The creep strength as well as the precipitation-strengthening contribution in the investigated Co-base superalloys increases with increasing γ' volume fraction reaching a maximum in VF60, the alloy with the highest investigated γ' volume fraction of 70 pct.
- While VF20 converges to a maximum precipitation-strengthening contribution of 121 MPa, the strengthening contributions in the alloys VF40 and VF60 exceed 340 and 510 MPa, respectively, but do not obtain a constant, maximum value at high-stress level.
- The precipitation-strengthening contribution of the γ'-Co_3(Al,W,Ta) phase in the Co-base superalloy VF60 at 1223 K (950 °C) ranges between the strengthening contributions of the γ' precipitates in the first- and second-generation Ni-base superalloys CMSX-6 and CMSX-4.
- The strengthening contribution of the γ'-Co_3(Al,W,Ta) phase is 73 MPa in VF20, 208 MPa in VF40, 307 MPa in VF60 according to the LBR approach compared to the strengthening contribution of the γ'-Ni_3(Al,Ta) phase of 216 MPa in CMSX-6 and 397 MPa in CMSX-4 at a minimum creep rate of 10^{-7} s^{-1} and at a temperature of 1223 K (950 °C).

ACKNOWLEDGMENTS

Open Access funding provided by Projekt DEAL. The authors acknowledge funding by the Deutsche Forschungsgemeinschaft (DFG) through project B3 of the Collaborative Research Center SFB/TR 103: "From Atoms to Turbine Blades—A Scientific Approach for Developing the Next Generation of Single Crystal Superalloys". One of the authors (FX) acknowledges funding by the Sino-German (CSC-DAAD) Postdoc Scholarship. One of the authors (CHZ) acknowledges funding by the Alexander von Humboldt Foundation (AvH) through a Feodor Lynen Research Fellowship.

OPEN ACCESS

APPENDIX A

CONVERSION OF THE STRENGTHENING CONTRIBUTION IN CMSX-6 TO 1223 K (950 °C)

The traditional power law equation describes the dependence of stress σ and temperature T on the minimum creep rate $\dot{\varepsilon}_{min}$:

$$\dot{\varepsilon}_{min} = A\sigma^n \exp\left(-\frac{Q_{app}}{RT}\right), \qquad [A1]$$

where A is a constant and Q_{app} is the apparent activation energy.

Solving Eq. [A1] for the stress σ and inserting the resulting expression for the precipitation-strengthened alloy and the matrix into Eq. [1] at temperature T_1 yields:

$$\sigma_{P,T_1}(\dot{\varepsilon}_{min}) = \sqrt[n_A]{\frac{\dot{\varepsilon}_{min}}{A_A \exp\left(\frac{-Q_{app,a}}{RT_1}\right)}} + \sqrt[n_M]{\frac{\dot{\varepsilon}_{min}}{A_M \exp\left(\frac{-Q_{app,m}}{RT_1}\right)}}, \qquad [A2]$$

where A_A, A_M are constants and n_A, n_M are the stress exponents of the precipitation-strengthened alloy and the matrix phase, respectively. Assuming n_A and n_M to be independent of temperature, which can be justified by the small temperature difference of only 30 K,

Eq. [A1] for the temperature T_2 can be inserted into Eq. [A2]:

$$\sigma_{\mathrm{P},T_1}(\dot{\varepsilon}_{\min}) = \left(\sigma_{A,T_2}(\dot{\varepsilon}_{\min}) \cdot \sqrt[n_\mathrm{A}]{\exp\left(\frac{-Q_{\mathrm{app,A}}}{R}\left(\frac{1}{T_2}-\frac{1}{T_1}\right)\right)}\right) - \left(\sigma_{\mathrm{M},T_2}(\dot{\varepsilon}_{\min}) \cdot \sqrt[n_\mathrm{M}]{\exp\left(\frac{-Q_{\mathrm{app,M}}}{R}\left(\frac{1}{T_2}-\frac{1}{T_1}\right)\right)}\right) \quad [A3]$$

Thus, only the apparent activation energies $Q_{\mathrm{app,A}}$ for the precipitation-strengthened alloy and $Q_{\mathrm{app,M}}$ for the matrix phase have to be known for the determination of the precipitation-strengthening contribution σ_P at a different temperature T_1, since n_A, n_M, σ_{A,T_2} and σ_{M,T_2} have already been determined at temperature T_2.

For CMSX-6, an apparent activation energies $Q_{\mathrm{app,A}}$of 797 kJ/mol is used as derived from the data of Wilhelm *et al.*[33] The apparent activation energy of the matrix phases $Q_{\mathrm{app,M}}$ can be estimated by the following equation[39].

$$Q_{\mathrm{app,M}} = Q_{\mathrm{Ni}} + \sum_n x_n Q_{n,\mathrm{Ni}}, \quad [A4]$$

where Q_{Ni} is the activation energy for self-diffusion of Nickel, x_n is the concentration of solute n and $Q_{n,\mathrm{Ni}}$ is the activation energy for interdiffusion of solute n in Nickel. Using the activation energies for interdiffusion determined in various binary Ni-X alloys,[40–44] the apparent activation energy equals approximately 423 kJ/mol for the matrix phase (Ni 51.1 at. pct, Al 3.1 at. pct, Co 20.3 at. pct, Cr 21.4 at. pct, Mo 0.9 at. pct, Ta 0.1 at. pct, Ti 0.1 at. pct, W 3.0 at. pct[33]).

REFERENCES

1. J. Sato, T. Omori, K. Oikawa, I. Ohnuma, R. Kainuma, and K. Ishida: *Science*, 2006, vol. 312, pp. 90–1.
2. S. Meher, H.-Y. Yan, S. Nag, D. Dye, and R. Banerjee: *Scr. Mater.*, 2012, vol. 67, pp. 850–53.
3. T. Omori, K. Oikawa, J. Sato, I. Ohnuma, U.R. Kattner, R. Kainuma, and K. Ishida: *Intermetallics*, 2013, vol. 32, pp. 274–83.
4. I. Povstugar, P.-P. Choi, S. Neumeier, A. Bauer, C.H. Zenk, M. Göken, and D. Raabe: *Acta Mater.*, 2014, vol. 78, pp. 78–85.
5. A. Suzuki and T.M. Pollock: *Acta Mater.*, 2008, vol. 56, pp. 1288–97.
6. A. Bauer, S. Neumeier, F. Pyczak, and M. Göken: *Scr. Mater.*, 2010, vol. 63, pp. 1197–200.
7. F. Xue, M. Wang, and Q. Feng: in *Superalloys 2012*, E.S. Huron, R.C. Reed, M.C. Hardy, M.J. Mills, R.E. Montero, P.D. Portella, and J. Telesman, eds., TMS, Warrendale, 2012, pp. 813–21.
8. A. Mottura, A. Janotti, and T.M. Pollock: *Intermetallics*, 2012, vol. 28, pp. 138–43.
9. M.S. Titus, A. Mottura, G. Babu Viswanathan, A. Suzuki, M.J. Mills, and T.M. Pollock: *Acta Mater.*, 2015, vol. 89, pp. 423–37.
10. M.S. Titus, A. Suzuki, and T.M. Pollock: in *Superalloys 2012*, Huron, E.S., Reed, R.C., Hardy, M.C., Mills, M.J., Montero, R.E., Portella, P.D., and Telesman, J., eds., TMS, Warrendale, 2012, pp. 823–32.
11. A. Bauer, S. Neumeier, F. Pyczak, R.F. Singer, and M. Göken: *Mater. Sci. Eng. A*, 2012, vol. 550, pp. 333–41.
12. A. Suzuki, G.C. DeNolf, and T.M. Pollock: *Scr. Mater.*, 2007, vol. 56, pp. 385–88.
13. K. Tanaka, M. Ooshima, N. Tsuno, A. Sato, and H. Inui: *Philos. Mag.*, 2012, vol. 92, pp. 4011–27.
14. F. Xue, H.J. Zhou, Q.Y. Shi, X.H. Chen, H. Chang, M.L. Wang, and Q. Feng: *Scr. Mater.*, 2015, vol. 97, pp. 37–40.
15. M.S. Titus, Y.M. Eggeler, A. Suzuki, and T.M. Pollock: *Acta Mater.*, 2015, vol. 82, pp. 530–9.
16. F. Xue, C.H. Zenk, L.P. Freund, M. Hoelzel, S. Neumeier, and M. Göken: *Scr. Mater.*, 2018, vol. 142, pp. 129–32.
17. M. Lenz, Y.M. Eggeler, J. Müller, C.H. Zenk, N. Volz, P. Wollgramm, G. Eggeler, S. Neumeier, M. Göken, and E. Spiecker: *Acta Mater.*, 2019, vol. 166, pp. 597–610.
18. T.M. Pollock and A.S. Argon: *Acta Metall. Mater.*, 1992, vol. 40, pp. 1–30.
19. N. Matan, D.C. Cox, P. Carter, M.A. Rist, C.M.F. Rae, and R.C. Reed: *Acta Mater.*, 1999, vol. 47, pp. 1549–63.
20. M. Feller-Kniepmeier and T. Link: *Metall. Trans. A*, 1989, vol. 20, pp. 1233–8.
21. R. Lagneborg and B. Bergman: *Met. Sci.*, 1976, vol. 10, pp. 20–8.
22. B. Reppich, M. Heilmaier, K. Liebig, G. Schumann, K.-D. Stein, and T. Woller: *Steel Res.*, 1990, vol. 61, pp. 251–57.
23. R. Lagneborg: *J. Mater. Sci.*, 1968, vol. 3, pp. 596–602.
24. P.W. Davies, G. Nelmes, K.R. Williams, and B. Wilshire: *Met. Sci. J.*, 1973, vol. 7, pp. 87–92.
25. O.D. Sherby and P.M. Burke: *Prog. Mater. Sci.*, 1968, vol. 13, pp. 323–90.
26. R. Lagneborg: *Scr. Metall.*, 1973, vol. 7, pp. 605–13.
27. W. Blum and B. Reppich: *Acta Metall.*, 1969, vol. 17, pp. 959–66.
28. A. Heckl, R. Rettig, and R.F. Singer: *Metall. Mater. Trans. A*, 2010, vol. 41A, pp. 202–11.
29. R. Bürgel, H.J. Maier, and T. Niendorf: *Handbuch Hochtemperatur-Werkstofftechnik*, 4th ed., Vieweg+Teubner Verlag, Wiesbaden, 2011.
30. R.C. Reed, N. Matan, D.C. Cox, M.A. Rist, and C.M.F. Rae: *Acta Mater.*, 1999, vol. 47, pp. 3367–81.
31. W. Schneider: Dr.-Ing. Dissertation, University of Erlangen–Nuremberg, 1993.
32. W. Schneider, J. Hammer, and Mughrabi, H.: in *Superalloys 1992*, Antolovich, S.D., MacKay, R.A., Anton, D.L., Khan, T., Kissinger, R.D., and Klarstrom, D.L., eds., TMS, Warrendale, 1992, pp. 589–98.
33. F. Wilhelm, E. Affeldt, E. Fleischmann, U. Glatzel, and J. Hammer: *Int. J. Fatigue*, 2017, vol. 97, pp. 1–8.
34. E. Fleischmann: Dr.-Ing. Dissertation, University of Bayreuth, 2013.
35. K. Kakehi: *Scr. Mater.*, 1999, vol. 41, pp. 461–5.
36. D.M. Knowles and S. Gunturi: *Mater. Sci. Eng. A*, 2002, vol. 328, pp. 223–37.
37. N. Tsuno, S. Shimabayashi, K. Kakehi, C.M.F. Rae, and R.C. Reed: in *Superalloys 2008*, TMS, Warrendale, 2008, pp. 433–42.
38. P. Lukáš, J. Čadek, V. Šustek, and L. Kunz: *Mater. Sci. Eng. A*, 1996, vol. 208, pp. 149–57.
39. Z. Zhu, H. Basoalto, N. Warnken, and R.C. Reed: *Acta Mater.*, 2012, vol. 60, pp. 4888–900.
40. M.S.A. Karunaratne, P. Carter, and R.C. Reed: *Mater. Sci. Eng. A*, 2000, vol. 281, pp. 229–33.
41. S.B. Jung, T. Yamane, Y. Minamino, K. Hirao, H. Araki, and S. Saji: *J. Mater. Sci. Lett.*, 1992, vol. 11, pp. 1333–7.
42. M.S.A. Karunaratne and R.C. Reed: *Defect Diffus. Forum*, 2005, vols. 237–240, pp. 420–5.
43. K. Monma, H. Suto, and H. Oikawa: *J. Jpn. Inst. Met.*, 1964, vol. 28, pp. 188–92.
44. M.S.A. Karunaratne, P. Carter, and R.C. Reed: *Acta Mater.*, 2001, vol. 49, pp. 861–75.